Geomechanics and Engineering, *Vol. 33, No. 3 (2023) 317-326*
https://doi.org/10.12989/gae.2023.33.3.317

A novel laboratory method for measuring the hydraulic conductivity of dredged slurry with high water contents

Cong Mou, Jian-wen Ding, Jian-hua Wang* and Xing Wan

Institute of Geotechnical Engineering, Transportation College, Southeast University, Nanjing 210096, China

(*Received September 15, 2022, Revised March 7, 2023, Accepted March 14, 2023*)

Abstract. Accurately measuring the hydraulic conductivity of dredged slurry (HCODS) is a difficult task and usually requires highly developed experimental techniques. To resolve such problem, this paper presents a novel laboratory method, where a double drainage sedimentation test (DDST) is proposed to generate a downward seepage after the end of primary consolidation (EOP). Based on the established stress equilibrium equations, it is figured out that the determination of local hydraulic gradients requires the effective stress distribution to be measured. Accordingly, an additional single drainage sedimentation test (SDST) with the same initial water content is performed in the novel laboratory method, which can be utilized to establish the relationship between effective stress and water content for investigated slurry. Thus, HCODS can be determined via a pair of SDST and DDST, with the water contents after the EOP measured. The corresponding calculation procedure is given in details. With a simply-designed settling column, the hydraulic conductivity tests were performed on three types of dredged slurry. The results demonstrated the effectiveness of the novel laboratory method in measuring HCODS.

Keywords: dredged slurry; hydraulic conductivity; laboratory method; sedimentation; test procedure

1. Introduction

A large amount of dredged slurry is generated annually in port and waterway projects, which is hard to directly utilize due to undesirable engineering properties, e.g., high water contents, high compressibility, and low strength (Bian *et al.* 2016, Develioglu and Pulat 2019, Dong *et al.* 2020, Kim *et al.* 2015, Lei *et al.* 2018, Wu *et al.* 2017, Yoobanpot *et al.* 2018). To dispose massive dredged slurry, it is commonly pumped into a large artificial storage yard to form reclaimed lands (Anda *et al.* 2020, Berilgen and Bulut 2016, Chian and Bi 2021, Karadoğan *et al.* 2021, Wu *et al.* 2019, Zeng *et al.* 2018). Hydraulic conductivity, which governs the dewatering behavior of dredged slurry, plays a key role in the design and settlement prediction of reclaimed lands filled with dredged slurry (Chen *et al.* 2019, De Lillis *et al.* 2020, Hossain and Chai 2014, Jun *et al.* 2021, Zeng *et al.* 2020a). Therefore, accurately measuring the hydraulic conductivity of dredged slurry (HCODS) is of great significance for dredging engineering.

According to Darcy's law, both seepage velocity and hydraulic gradient need to be measured to calculate hydraulic conductivity in permeability tests. At present, however, measuring HCODS is still a challenge, because of the extremely high compressibility of dredged slurry. For measuring HCODS via common permeability tests, e.g., constant head test, falling head test, and flow pump test, two serious problems can be encountered (Pane and Schiffman 1997): (1) imposed hydraulic gradient and seepage can induce consolidation and large volume change of slurry specimen; (2) highly non-uniform distribution of void ratio within the specimen can be caused by its self-weight. To overcome such problems, some model test methods were proposed, where void ratios and hydraulic conductivities at different heights are determined. Utilizing an X-ray technique and pore pressure transducers, Been and Sills (1981) measured the densities and pore water pressures within the slurry specimen during self-weight consolidation. With the measured data, the velocity of upward seepage induced by the buoyant weight of soil particles, hydraulic gradients, and then hydraulic conductivities could be calculated. Different from Been and Sills (1981), Imai (1979) proposed a seepage-induced consolidation (SIC) test, where a semiautomatic system applying a constant hydraulic head difference instead of the specimen's self-weight was used to generate a downward seepage. After the end of primary consolidation (EOP), the steady seepage velocity, water content distribution, and pore water pressure distribution were measured to determine HCODS. However, these model test methods have not been widely used in practice, because the reliable measurement of pore pressures within slurry specimens is a difficult task and requires a highly developed experimental technique (Fox and Baxter 1997).

It is worth noting that some ideas from the model tests (Imai 1979, Been and Sills 1981) are still enlightening, which are: (1) seepage can be generated by utilizing the self-weight of the specimen; (2) using steady state (i.e., the state after the EOP) to calculate hydraulic conductivity involves less computational efforts than the use of transient part; (3) the data (e.g., seepage velocity, water content

*Corresponding author, Research Associate
E-mail: jianhua_wang@seu.edu.cn
[a]Ph.D. Candidate
E-mail: congmou@seu.edu.cn

ISSN: 2005-307X (Print), 2092-6219 (Online)

distribution and so on) after the EOP is convenient to measure. Therefore, a double drainage sedimentation test (DDST), in which a downward seepage is induced by the self-weight of the specimen after the EOP, can significantly facilitate the measurement of HCODS. Besides, to determine the inner stress distribution without directly measuring pore pressures, a single drainage sedimentation test (SDST) with the same initial water content needs to be performed. The SDST can be utilized to figure out the relationship between water content and effective stress for investigated slurry with a specific water content (Hong *et al.* 2010, Imai 1981, Zeng *et al.* 2020b). Consequently, the stress distribution within the DDST specimen can be determined with the measured water contents of a pair of SDST and DDST specimens.

In this study, a novel laboratory method for measuring HCODS is proposed, where a pair SDST and DDST with the same initial water contents require to be performed. The stress state after the EOP for both SDST and DDST specimens are analyzed. Based on the established stress equilibrium equations, the procedure for determining HCODS is described in details as well as the limitations and solutions. Furthermore, tests on three types of dredged slurry were performed with a simply-designed settling column. The hydraulic conductivities of investigated slurry are calculated and verified.

2. Theoretical basis

2.1 Basic assumption

To determine hydraulic conductivity via a pair SDST and DDST, the following assumptions are considered:

(1) Dredged slurry is homogeneous and saturated;

(2) The soil particles and water in dredged slurry are incompressible;

(3) Darcy's law is valid;

(4) The effect of secondary consolidation is ignored.

2.2 Principle

Fig. 1 shows the typical schematic diagrams of SDST and DDST specimens. The bottom boundary of the SDST specimen is impermeable, while the bottom boundary of the DDST specimen is permeable.

Before the EOP, there is only the upward seepage due to the buoyant weight of soil particles in SDST; while in DDST, there is a downward seepage besides the upward seepage. Fig. 2 shows the schematic diagrams of the sedimentation process for the DDST specimen. Because of the upward seepage, the drop rate of water surface is smaller than that of slurry surface before the EOP. The upward discharged water lies above the slurry. After the EOP, the buoyant weight of soil particles is totally counterbalanced by the effective stress, the upward seepage does not occur any more, and there still exists the downward seepage generated by the weight of water, as shown in Fig. 2. The velocity of the downward seepage equals the drop rate of water surface, which is easy to

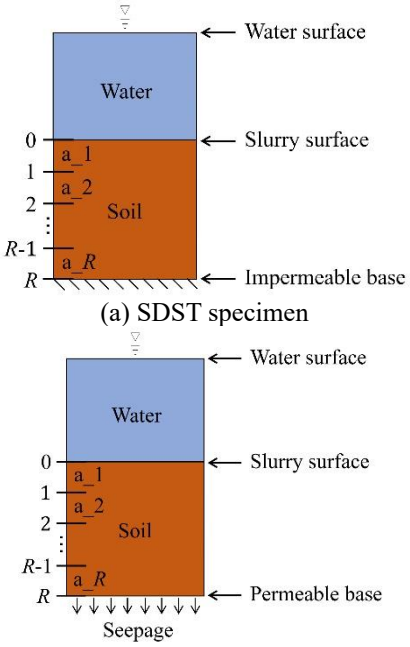

Fig. 1 Typical schematic diagrams of SDST and DDST specimens

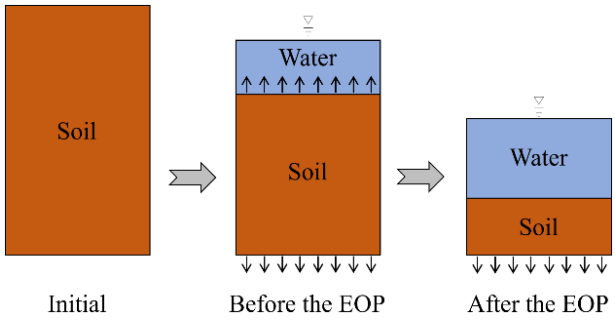

Fig. 2 Typical schematic diagrams of the sedimentation process for the DDST specimen

measure. Hence, the key to determining hydraulic conductivity is accurately determining the hydraulic gradient distribution within the DDST specimen, the principle of which is clarified in the following.

Fig. 3 shows the stress state of an element in a specimen after the EOP. The coordinate direction is the same as the gravity direction. The element has a thickness of dx. The vertical equilibrium of the element requires that

$$-\frac{\partial \sigma}{\partial x}+\gamma_{\mathrm{s}}(1-n)+\gamma_{\mathrm{w}} n=0 \tag{1}$$

where, σ is the vertical total stress; n is the porosity; γ_{s} is the unit weight of soil particles; γ_{w} is the unit weight of water. According to the effective stress principle,

$$\frac{\partial \sigma}{\partial x}=\frac{\partial \sigma^{\prime}}{\partial x}+\frac{\partial u}{\partial x} \tag{2}$$

where $\sigma^{\prime}$ is the effective stress and u is the pore water pressure. Before the EOP, because slurry is saturated and consists of only soil particles and water, according to the

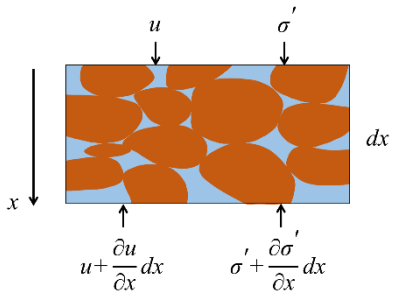

Fig. 3 Stress state of an element in a specimen after the EOP

cause of pore water pressure, u can be expressed as

$$u = u_w + u_s \tag{3}$$

where, u_w is the pore water pressure caused by the weight of water; u_s is the (excess) pore water pressure caused by the buoyant weight of soil particles. After the EOP, u_s is dissipated to be zero (Imai 1979, 1981), and hence $u = u_w$. Then the following equation can be yielded

$$-\frac{\partial \sigma'}{\partial x} - \frac{\partial u_w}{\partial x} + \gamma_s(1-n) + \gamma_w n = 0 \tag{4}$$

Eq. (4) can be regarded as the stress equilibrium equation after the EOP for the soil skeleton of the SDST specimen or the DDST specimen. The difference between them lies in the value of $\frac{\partial u_w}{\partial x}$, which represents the effect of the weight of water on soil skeleton.

For the SDST specimen, $\frac{\partial u_w}{\partial x}$ is known to be γ_w. And the following equation can be obtained by substituting $\frac{\partial u_w}{\partial x} = \gamma_w$ into Eq. (4):

$$\frac{\partial \sigma'}{\partial x} = (\gamma_s - \gamma_w)(1-n) \tag{5}$$

where $(\gamma_s - \gamma_w)(1-n)$ is the buoyant unit weight of soil skeleton under the hydrostatic condition.

While for the DDST specimen, $\frac{\partial u_w}{\partial x}$ is unknown and is associated with seepage force. In the case where $\frac{\partial u_w}{\partial x} > 0$, the weight of water in the element does not totally serve as seepage force, and the soil skeleton in the element is affected by the upward buoyancy of water. Then Eq. (4) can be written as

$$\frac{\partial \sigma'}{\partial x} = (\gamma_s - \frac{\partial u_w}{\partial x})(1-n) + \gamma_w n - n\frac{\partial u_w}{\partial x} \tag{6}$$

where, $\gamma_w n - n\frac{\partial u_w}{\partial x}$ is seepage force; $(\gamma_s - \frac{\partial u_w}{\partial x})(1-n)$ is the buoyant unit weight of soil skeleton. Note that the buoyant unit weight here is different from the one under the hydrostatic condition in value. $\frac{\partial u_w}{\partial x}$ here should be between 0 and γ_w.

In the other case where $\frac{\partial u_w}{\partial x} \le 0$, the weight of water in the element totally serves as downward seepage force, and the water in the element has no buoyancy effect on the soil skeleton. Then Eq. (4) can be written as

$$\frac{\partial \sigma'}{\partial x} = \gamma_s(1-n) + \gamma_w n - \frac{\partial u_w}{\partial x} \tag{7}$$

where, $\gamma_w n - \frac{\partial u_w}{\partial x}$ is seepage force; $\gamma_s(1-n)$ is the dry unit weight of soil skeleton. Although Eqs. (6) and (7) are identical in form, the physical meanings of $-\frac{\partial u_w}{\partial x}(1-n)$ in two equations are different. In Eq. (6), $-\frac{\partial u_w}{\partial x}(1-n)$ presents as buoyancy, while in Eq. (7), $-\frac{\partial u_w}{\partial x}(1-n)$ presents as seepage force.

Eq. (5) reflects the relationship between the effective stress distribution and the water content distribution of the SDST specimen. Eqs. (6) and (7) reflect the relationship between the effective stress distribution, local seepage force, and the water content distribution of the DDST specimen, where $\frac{\partial u_w}{\partial x}$ is associated with seepage force. If $\frac{\partial u_w}{\partial x}$ can be calculated, the seepage force and then hydraulic gradient can be determined. According to Eq. (4), $\frac{\partial u_w}{\partial x}$ is relevant to σ' and n. For the DDST specimen, n is easy to obtain with the measured water contents, however, σ' is difficult to directly calculate. Luckily, it has been demonstrated that the compression behavior of dredged slurry is governed by the liquid limit and the initial water content (Hong *et al.* 2010, 2012, Zeng *et al.* 2015, 2020b), i.e., the relationship between σ' and e (void ratio) of the specific dredged slurry with a specific initial water content is unique. Therefore, σ' within the DDST specimen can be determined by the interpolation of the σ'-e relationship obtained with the water content distribution of the SDST specimen and Eq. (5). Then $\frac{\partial u_w}{\partial x}$ and hydraulic gradients at different heights can be calculated based on Eqs. (6) and (7). Fig. 4 clearly shows how the hydraulic gradient distribution of the DDST specimen can be determined with the water content distribution of a pair of SDST and DDST specimens.

2.3 Procedure for calculating hydraulic conductivity

To clarify how to calculate k (hydraulic conductivity) step by step with measured data, the notations of measured data need to be illustrated. As shown in Fig. 1, from top to bottom, different sampling points of a specimen are marked

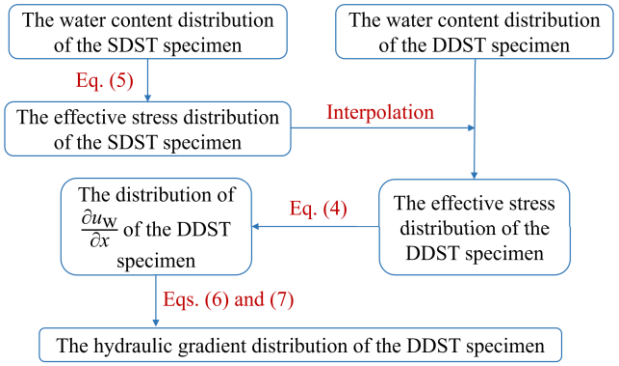

Fig. 4 Flow chart of determining the hydraulic gradient

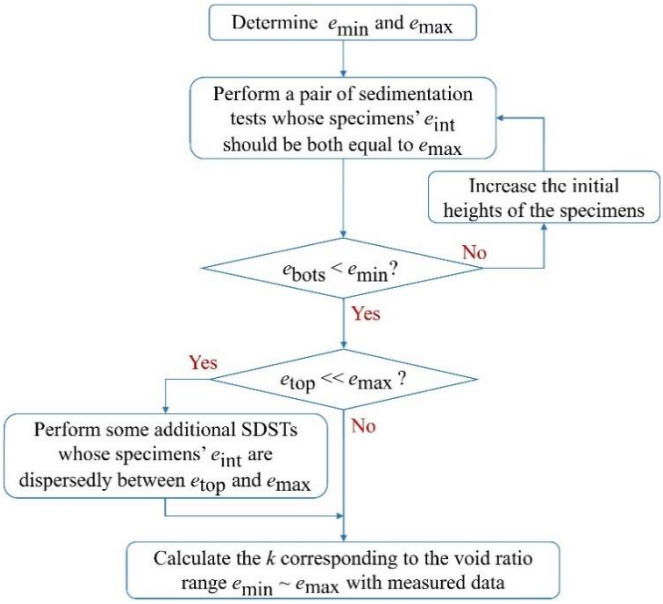

Fig. 5 Flow chart of the procedure for determining HCODS corresponding to an arbitrary void ratio range

with r ($r = 0, 1, 2, \ldots, R$), and soil layers between two adjacent sampling points are marked with a_r ($r = 1, 2, \ldots, R$). For examples, w_r is the water content of the soil at the sampling point r, while w_{a_r} is the average water content of the soil layer between sampling point $r - 1$ and sampling point r; H_r is the height of point r, while ΔH_{a_r} is the thickness of the soil layer between sampling point r - 1 and sampling point r, and so on. The calculation of k can be conducted by the following four steps:

(1) n_r and n_{a_r} within the SDST specimen can be easily calculated with measured water content distribution. Then σ_r' within the SDST specimen can be calculated by integrating Eq. (5)

$$\sigma_r' = \int_0^{H_r} (\gamma_s - \gamma_w)(1 - n)\mathrm{d}x \tag{8}$$

The calculated e_r-σ_r' relation reflects the compression behavior of the investigated dredged slurry with a specific initial water content.

(2) σ_r' and $\frac{\partial \sigma'}{\partial x}|_{a\_r}$ within the DDST specimen can be determined by the interpolation of the e_r - σ_r' relation obtained in step (1). Then $\frac{\partial u_w}{\partial x}|_{a\_r}$ can be calculated by substituting $\frac{\partial \sigma'}{\partial x}|_{a\_r}$ into Eq. (4).

(3) If $\frac{\partial u_w}{\partial x}|_{a\_r} > 0$, based on Eq. (6), the average hydraulic gradient of the soil layer i_{a_r} can be calculated by

$$i_{a\_r} = n_{a\_r} - \frac{n_{a\_r}}{\gamma_w}\frac{\partial u_w}{\partial x}|_{a\_r} \tag{9}$$

If $\frac{\partial u_w}{\partial x}|_{a\_r} \le 0$, based on Eq. (7), i_{a_r} can be calculated by

$$i_{a\_r} = n_{a\_r} - \frac{1}{\gamma_w}\frac{\partial u_w}{\partial x}|_{a\_r} \tag{10}$$

(4) In DDST, the measured seepage velocity at the EOP v_{wem} can be easily obtained with the curve of water surface height with time. Then, according to Darcy's law, the average hydraulic conductivity of a soil layer k_{a_r} can be calculated with

$$k_{a\_r} = \frac{v_{wem}}{i_{a\_r}} \tag{11}$$

The determined e_{a_r} - k_{a_r} relationship reflects the permeability behavior of the investigated dredged slurry. Note that e_{a_r} and k_{a_r} are the average values of one soil layer. Therefore, the smaller the distance between two adjacent sampling points, the more accurate the determined k-e relationship.

2.4 Limitations and solutions

It needs to be noted that, when it comes to permeability test, the commonly expected test result is a curve of k with e plotted by connecting measured data points. The curve needs to satisfy the following two requirements: (1) the range of the curve should cover the range of the needed k-e relationship; (2) any two adjacent data points should be close enough so that the curve is smooth and can accurately reflect the permeability behavior of investigated slurry.

Let e_{min} and e_{max} respectively denote the lower limit and the upper limit of the e for the k-e relationship needed to be determined. For both SDST and DDST specimens, the maximum e after the EOP is the void ratio at the top surface e_{top} theoretically, and there must be that $e_{top} \le e_m$, where e_m is the soil-formation void ratio (Been and Sills 1981, Xu *et al.* 2012). Therefore, the novel laboratory method is only applicable to measure the k corresponding to the e less than e_m. If there is the need to measure the k corresponding to the e greater than e_m, i.e., $e_m < e_{max}$, the method proposed by Pane and Schiffman (1997) can be used in combination with the novel test method proposed in this paper. In SDST,

if the initial void ratio e_{int} is larger than e_m, zone settling will occur in the upper area, where effective stress is zero. In such case, Pane and Schiffman (1997) suggested that the hydraulic conductivity at the initial void ratio $k(e_{int})$ can be calculated by

$$k(e_{int}) = \frac{v_{si}(1 + e_{int})}{G_s - 1} \tag{12}$$

where v_{si} and G_s are the initial settling velocity and specific gravity of soil particles respectively.

The lower limit of the e for the k-e relationship able to be measured via the novel test method is the bottom void ratio of the SDST specimen e_{bots}, because the σ' at the e less than e_{bots} cannot be obtained. Without the σ'-e relationship of investigated dredged slurry, whether e_{bots} is less than e_{min} cannot be known before the tests. Hence, a pair of tests (an SDST and a DDST) need to be conducted first based on experimental experience, and the e_{int} of the two specimens should be both equal to e_{max}. If the measured e_{bots} is larger than e_{min}, the initial heights of the two specimens should be increased until $e_{bots} < e_{min}$.

Furthermore, if e_{max} is much larger than e_m, there will be that $e_{top} << e_{max}$. Under such circumstance, to make the finally obtained k-e curve smooth enough, some SDSTs whose specimens' e_{int} are dispersedly between e_{top} and e_{max} should be additionally performed. It can be seen from Eq. (12) that only the initial settling velocity v_{si} needs to be measured to obtain $k(e_{int})$. Hence, the additional SDSTs do not require much experimental work.

According to the above procedure, the HCODS corresponding to an arbitrary void ratio range can be measured. Fig. 5 shows the flow chart of the procedure.

3. Hydraulic conductivity test

3.1 Apparatus

An experimental apparatus was simply designed to verify the proposed laboratory method, based on the above principle. Fig. 6 shows the schematic diagram of the experimental apparatus, which mainly consists of an acrylic cap, an acrylic settling column, a porous stone, and three stainless valves. The acrylic settling column is equipped with measuring scales on the flank to measure the heights of the slurry surface and water surface. The settling column has a height of 30 cm and an inner diameter of 18 cm which is large enough to ignore the frictional effect of the column's inner wall on settling behavior (Gao *et al.* 2016). Three stainless valves are dispersedly installed at the same height as the porous stone. By opening or closing the valves, the drainage condition turns to be double or single. The acrylic cap can prevent the evaporation of water, and a small hole is drilled in its center to make the air pressure at the top and the bottom of the DDST specimen equal.

3.2 Materials

Tests were performed on three types of dredged slurry,

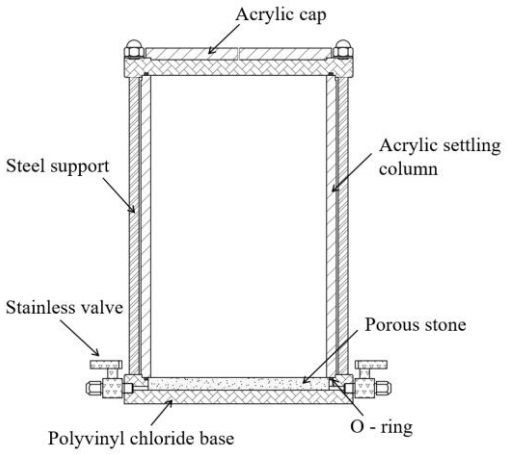

Fig. 6 Schematic diagram of experimental apparatus

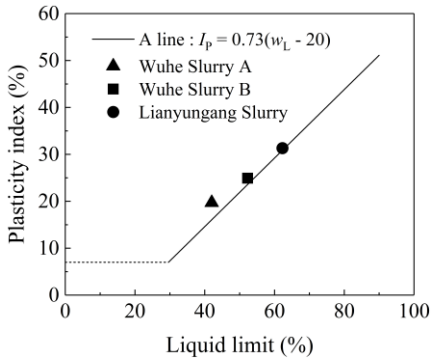

Fig. 7 Plasticity chart

termed Wuhe slurry A, Wuhe slurry B and Lianyungang slurry respectively. The samples of Wuhe slurry A and Wuhe slurry B were taken from the reclaimed area created by the dredged slurry from the Xiangmiao-Fushan section of Huaihe River in China. The samples of Lianyungang slurry were taken from a reclaimed area near Liezikou Bridge in Lianyungang city, Jiangsu province, China. Table 1 shows the basic physical properties of three types of dredged slurry. The liquid limit w_L and plastic limit w_P were measured by using the Casagrande method and rolling method respectively. Fig. 7 shows the plasticity chart of investigated slurry, indicating that all slightly lie above the A-line defined by $I_P = 0.73(w_L - 20)$, where I_P is the plasticity index.

3.3 Testing program

Total eight self-weight sedimentation tests were performed. The testing program is shown in Table 2, where H_{int} and w_{int} are initial height and initial water content respectively.

Dredged slurry was prepared by being mixed with distilled water and stirred repeatedly. Then dredged slurry with the target w_{int} was put into the settling column. After the preparation of a specimen, slurry surface height was measured immediately and the three valves in DDST were opened. The time of preparing a pair of specimens should be close to ensure the same initial water contents. Slurry

Table 1 Basic physical properties of dredged slurry

Dredged slurry	Liquid limit (%)	Plastic limit (%)	Specific gravity	Clay (<0.005 mm, %)	Silt (0.005-0.075 mm, %)	Sand (0.075-2 mm, %)
Wuhe slurry A	42.0	22.3	2.71	52.0	46.6	1.4
Wuhe slurry B	52.3	27.4	2.74	67.5	32.3	0.2
Lianyungang slurry	62.3	31.0	2.72	74.0	25.9	0.1

Table 2 Testing program

Dredged slurry	Serial number	Drainage condition	H_{int} (cm)	w_L (%)	w_{int} / w_L
Wuhe slurry A	WSA-SD-W10	Single	29.2	42.0	10.0
	WSA-DD-W10	Double	29.0	42.0	10.0
Wuhe slurry B	WSB-SD-W8	Single	28.1	52.3	8.0
	WSB-DD-W8	Double	28.4	52.3	8.0
	WSB-SD-W10	Single	28.1	52.3	10.0
	WSB-SD-W12	Single	28.3	52.3	12.0
Lianyungang slurry	LS-SD-W10	Single	29.1	62.3	10.0
	LS-DD-W10	Double	28.6	62.3	10.0

surface height was measured in both SDST and DDST. While water surface height was measured only in DDST. When the reduction rate of slurry surface height slowed down abruptly, i.e., a clear inflexion point in the settlement curve is observed, the primary consolidation was considered completed as suggested by Imai (1981). Then the valves in DDST were closed.

To measure the water content distribution after the EOP, soils at different heights were sampled with a spoon layer by layer, i.e., each soil layer was removed after the sampling so that the lower soils could be sampled. Note that the water contents of the upper part of slurry specimen were still high after the EOP. The removal of the soil layers with a spoon would disturb the structure of lower soils and change their water contents. With a reference to the multilayer extraction sampling method used by Zhang *et al.* (2017), it is known that removing soils by suction would not disturb surrounding soils. Hence, a syringe with a hose attached was used in the tests to remove the soil layers having been sampled as well as the water above the slurry surface. While for the lower part of slurry specimen whose water contents were relatively low, the spoon was directly used to remove the soils. The corresponding heights were recorded precisely when sampling. Data of vertical distribution of water contents can be checked according to the mass conservation of water. It should be noted that the volume expansion of the DDST specimen due to the removal of seepage force was ignored in the measurement of the water content distribution as with the SIC test (Imai 1979).

3.4 Results

3.4.1 Slurry and water surface heights with time

Fig. 8 shows the curves of slurry and water surface heights with time for three pairs of SDST and DDST specimens. Despite the same w_{int}, the settlement rate of the

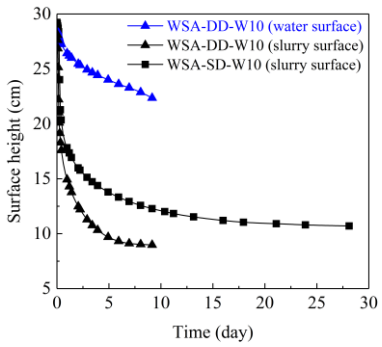

(a) Wuhe slurry A

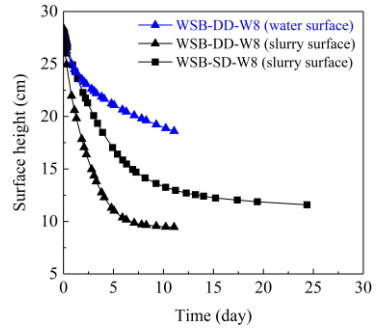

(b) Wuhe slurry B

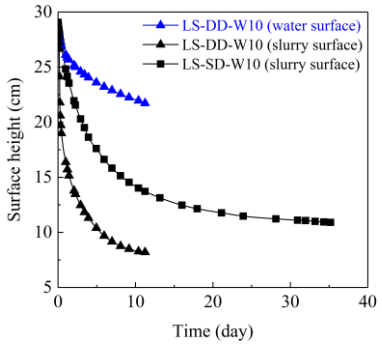

(c) Lianyungang slurry

Fig. 8 Curves of water and slurry surface heights with time for three pairs of specimens

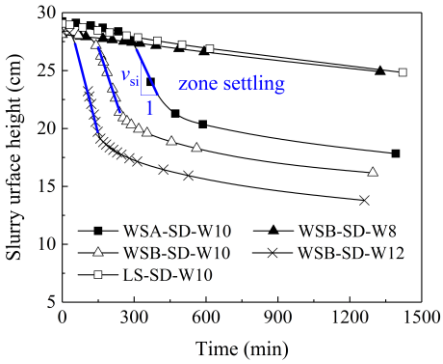

Fig. 9 Curves of slurry surface height with time for SDST specimens in the first 1500 min

Table 3 The check for measured water contents

Serial number	V_{wi} (cm)	V_{wm} (cm)	D_{wmi} (%)
WSA-SD-W10	26.84	26.76	0.34
WSA-DD-W10	26.68	26.42	0.97
WSB-SD-W8	25.84	25.39	1.74
WSB-DD-W8	26.12	25.50	2.37
LS-SD-W10	27.48	26.88	2.18
LS-DD-W10	27.01	26.61	1.48

DDST specimen is found significantly faster than that of the corresponding SDST specimen, and the final settling volume of the DDST specimen is also larger. The downward seepage force in DDST should be responsible for the difference.

In DDST, the drop rate of water surface gradually decreases with time, due to the reduction of hydraulic conductivity and total hydraulic head difference. Furthermore, because there exists the upward seepage besides downward seepage in DDST, the drop rate of water surface is smaller than that of slurry surface, which results in the accumulation of water on the slurry surface. After the EOP, slurry surface height almost remains constant, and the variation of water surface height with time is approximately linear, which makes v_{wem} easy to determine.

As noted above, if $e_{int} > e_m$, zone settling (also referred to as hindered settling) will occur in SDST, which can be identified according to the shape of the curve of slurry surface height with time (Xu *et al.* 2012, Zhang *et al.* 2017). Fig. 9 shows the curves of slurry surface height with time for five SDST specimens in the first 1500 min. The settling velocities of WSA-SD-W10, WSB-SD-W10 and WSB-SD-W12 are significantly higher than that of the other two specimens and exhibit abrupt drops, demonstrating the occurrence of zone settling. The corresponding $k(e_{int})$ of the three specimens can be determined with Eq. (12) consequently.

3.4.2 Water content distribution after the EOP

Fig. 10 shows the water content distribution after the EOP for three pairs of SDST and DDST specimens, where depth is the vertical distance downward from slurry surface. According to the mass conservation, the measured water

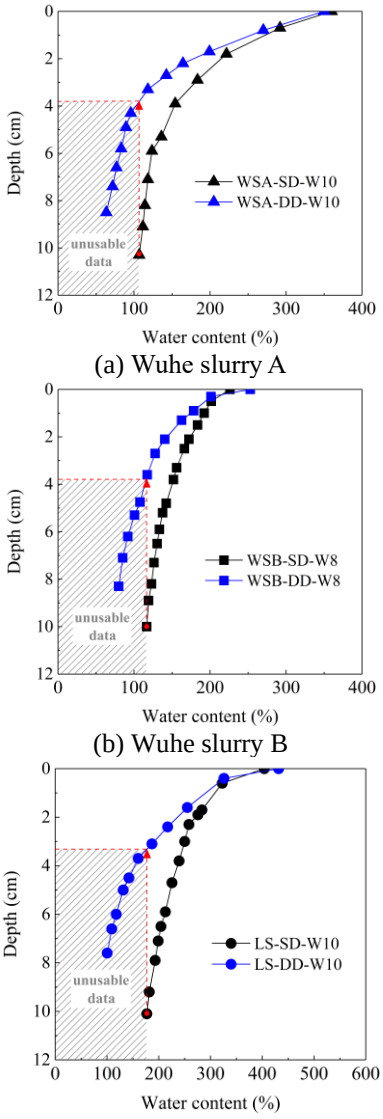

(a) Wuhe slurry A

(b) Wuhe slurry B

(c) Lianyungang slurry

Fig. 10 Water content distribution after the EOP

volume after the EOP should be the same with the initial water volume, which can help check the measured results of water content distribution. The initial water volume per unit area V_{wi} can be calculated with

$$V_{wi} = H_{int}\frac{e_{int}}{1+e_{int}} \tag{13}$$

The measured water volume per unit area V_{wm} after the EOP can be calculated with

$$V_{wm} = H_{int} - H_{seop} + \sum_{r=1}^{R} n_{a\_r}\Delta H_{a\_r} \tag{14}$$

where H_{seop} is the slurry surface height at the EOP. Then the deviation of V_{wm} relative to V_{wi} can be expressed as

$$D_{wmi} = \frac{|V_{wm} - V_{wi}|}{V_{wi}} \times 100\% \tag{15}$$

which reflects the accuracy of measured water contents for

a whole specimen. The values of D_{wmi} for three pairs of SDST and DDST specimens are listed in Table 3. All are within 2.37%, indicating that the way of sampling and measuring water contents after the EOP in this study is reliable.

From Fig. 10, it can be found that the water contents at the slurry surface of a pair of SDST and DDST specimens are basically the same. The difference between them gradually increases with increasing depth, which is attributed to the downward seepage force in DDST. The bottom water content of the DDST specimen is significantly smaller than that of the SDST specimen. Hence, for the lower part of the DDST specimen, where e is less than e_{bots}, the corresponding σ' cannot be obtained by interpolation and the water content distribution of this part cannot be used for determining k, as shown in Fig. 10.

4. Determination and verification of hydraulic conductivity

4.1 Determination of hydraulic conductivity

Pane and Schiffman (1997) suggested that a power equation can be employed to describe the k-e relationship of soft soils and slurry effectively in a wide range of void ratios. Therefore, the sedimentation test method proposed by Pane and Schiffman (1997), as described in section 2.4, can be regarded as a reference for the novel laboratory method proposed in this paper. If the results obtained by two methods can be described by a unified power function, the hydraulic conductivities determined by the novel laboratory method can be considered accurate.

According to the procedure for calculating k in section 2.3, the hydraulic conductivities of three types of dredged slurry are determined with the measured data shown in section 3.4. Fig. 11 shows the k-e relationships determined via two methods. Note that because no zone settling occurred in the SDST for Lianyungang slurry, only the novel laboratory method was used in determining the k-e relationship of Lianyungang slurry. Fig. 11 indicates that there exists a linear relationship between k and e in the double logarithmic coordinate, i.e., k is relevant to e in a power function. The k-e relationships of Wuhe slurry A, Wuhe slurry B, and Lianyungang slurry approximately satisfy the power functions $\frac{k}{\text{cm/s}} = 5 \times 10^{-7} e^{3.66}$, $\frac{k}{\text{cm/s}} = 4 \times 10^{-7} e^{3.74}$, and $\frac{k}{\text{cm/s}} = 5 \times 10^{-8} e^{4.18}$, which are illustrated by the solid lines in Fig. 11. And the corresponding variances are 0.976, 0.979 and 0.935 respectively. The slight fluctuation of data points should be ascribed to the small inaccuracies caused by the instability of manual sampling to measure water content distribution. Considering the significance of water contents in the novel laboratory method, some improvements in the measurement of water content distribution after the EOP may be made in the future.

4.2 Verification of hydraulic conductivity

The aim of this study is to provide a laboratory method

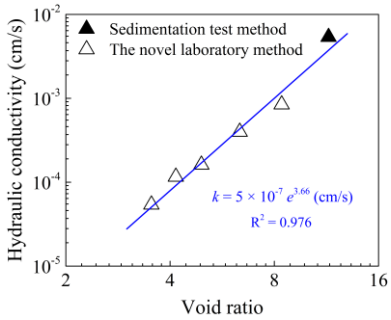

(a) Wuhe slurry A

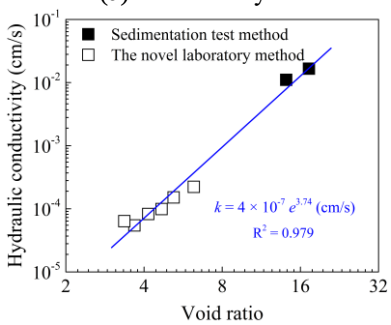

(b) Wuhe slurry B

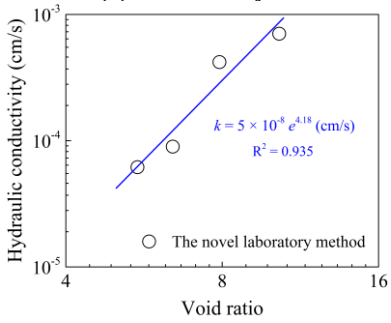

(c) Lianyungang slurry

Fig. 11 The k-e relationships of three kinds of dredged slurry

for measuring HCODS with low requirements for experimental techniques. Therefore, it is not practical for users to verify the results obtained via the novel laboratory method by comparing it with the test methods proposed by Imai (1979) or Been and Sills (1981) which require highly developed experimental techniques. One effective way for the verification is to compare the results obtained via the novel laboratory method with the ones obtained via the sedimentation test method proposed by Pane and Schiffman (1997), as shown in section 4.1, although it requires additional experimental work. In this section, another way to verify the hydraulic conductivities is provided as follows.

The seepage velocity at the EOP in DDST can not only be directly obtained with the measured curve of water surface height with time but also be calculated with the determined k-e relationship, because the average hydraulic gradient and the average hydraulic conductivity of the whole DDST specimen can be calculated if the k-e relationship is known. Let v_{wec} denote the seepage velocity at the EOP calculated with the determined k-e relationship.

If the difference between v_{wec} and measured v_{wem} is small, the determined hydraulic conductivity can be

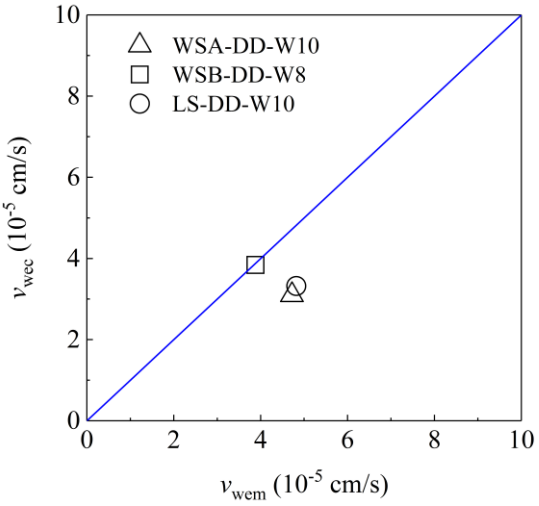

Fig. 12 The comparison between v_{wem} and v_{wec}

considered accurate. The calculation of v_{wec} can be conducted by the following three steps:

(1) With the determined k-e relationship, the average hydraulic conductivity $\overline{k}$ of the whole DDST specimen can be calculated by

$$\overline{k} = H_{seop} / \sum_{r=1}^{R} \left(\frac{\Delta H_{a\_r}}{k_{a\_r}} \right) \tag{16}$$

(2) The total hydraulic head difference between the top and the bottom of the DDST specimen can be calculated with

$$\Delta h = \left(H_{weop} - H_{seop} \right) + \sum_{r=1}^{R} \left(\Delta H_{a\_r} n_{a\_r} \right) + \Delta h' \tag{17}$$

where, H_{weop} is the water surface height at the EOP of the DDST specimen; $\Delta h'$ is the hydraulic head difference caused by the force (counterforce of buoyancy) of partial soil skeleton (where $\frac{\partial u_w}{\partial x} \geq 0$) on water, which can be calculated by

$$\Delta h' = \frac{1}{\gamma_w} \int \frac{\partial u_w}{\partial x} (1 - n) \mathrm{d}x \quad \text{for} \quad \frac{\partial u_w}{\partial x} \geq 0 \tag{18}$$

However, the values of $\Delta h'/\Delta h$ of WSA-DD-W10, WSB-DD-W8 and LS-DD-W10 can be calculated to be 2.6%, 3.0% and 1.7% respectively, indicating that $\Delta h'$ is negligible compared with Δh.

(3) Then v_{wec} can be calculated with

$$v_{wec} = \overline{k} \frac{\Delta h}{H_{seop}} \tag{19}$$

Fig. 12 shows the comparison between v_{wem} and v_{wec} for three DDST specimens. The difference between v_{wem} and v_{wec} is very small, demonstrating that the above determined v_{wem} and k-e relationships are accurate and the novel laboratory method is reliable to be used for measuring the hydraulic conductivity of dredged slurry with high water contents.

5. Conclusions

A novel laboratory method for measuring the hydraulic conductivity of dredged slurry with high water contents is proposed in this study. The main conclusions can be summarized as:

- The stress equilibrium equations under both single and double drainage conditions are established. It is revealed that the water content distribution of the SDST specimen after the EOP is only related with the effective stress; while for the DDST specimen, the water content distribution after the EOP is related with not only the effective stress but also the local seepage force induced by the weight of water. Based on the established theorical equations, the procedure for calculating hydraulic conductivity with measured water contents of a pair of SDST and DDST specimens is given.
- Hydraulic conductivity tests were performed on three types of dredged slurry with a simply-designed settling column, whose bottom boundary can be controlled to be either permeable or impermeable. The results demonstrated that the novel laboratory method is effective in measuring the hydraulic conductivity of dredged slurry.
- The novel laboratory method for measuring the hydraulic conductivity of dredged slurry via a pair of SDST and DDST does not require highly developed experimental techniques and equipment, e.g., pore pressure transducers with high accuracy or any semiautomatic system. Hence, it has the potential to be widely used in practical application.

Acknowledgments

The research described in this paper was financially supported by the National Natural Science Foundation of China (Grant numbers 41977243, 52278334, and 51978159) and the International Postdoctoral Exchange Fellowship Program from China Postdoctoral Council (Grant number PC2021016). The authors would like to express appreciation to the reviewers for their valuable comments and suggestions that helped to improve the quality of the paper.

References

Anda, R., Fu, H., Wang, J., Lei, H., Hu, X., Ye, Q., Cai, Y. and Xie, Z. (2020), "Effects of pressurizing timing on air booster vacuum consolidation of dredged slurry", *Geotext. Geomembranes*, **48**(4), 491-503. https://doi.org/10.1016/j.geotexmem.2020.02.007.

Been, K. and Sills, G.C. (1981), "Self-weight consolidation of soft soils: an experimental and theoretical study", *Geotechnique*, **31**(4), 519-535. https://doi.org/10.1680/geot.1981.31.4.519.

Berilgen, S.A. and Bulut, B.T. (2016), "Laboratory investigations for dewatering of golden horn dredged sludge with geotextile tubes", *Mar. Georesour. Geotechnol.*, **34**(7), 638-647. https://doi.org/10.1080/1064119X.2015.1068894.

Bian, X., Wang, Z.F., Ding, G.Q. and Cao, Y.P. (2016), "Compressibility of cemented dredged clay at high water content with super-absorbent polymer", *Eng. Geol.*, **208**, 198-

205. https://doi.org/10.1016/j.enggeo.2016.04.036.
Chen, B., Sun, D.A. and Jin, P. (2019), "Experimental study of the effect of microstructure on the permeability of saturated soft clays", *Geomech. Eng.*, **18**(1), 49-58. https://doi.org/10.12989/gae.2019.18.1.049.
Chian, S.C. and Bi, J. (2021), "Influence of grain size gradation of sand impurities on strength behaviour of cement-treated clay", *Acta Geotech.*, **16**(4), 1127-1145. https://doi.org/10.1007/s11440-020-01090-9.
De Lillis, A., Rotisciani, G.M. and Miliziano, S. (2020), "Numerical investigation of the behaviour of hydraulically dredged fine-grained soils during and after filling of the containment facility of the port of Gaeta", *Geotext. Geomembranes*, **48**(4), 591-601. https://doi.org/10.1016/j.geotexmem.2020.03.005.
Develioglu, I. and Pulat, H.F. (2019), "Compressibility behaviour of natural and stabilized dredged soils in different organic matter contents", *Constr. Build. Mater.*, **228**, 116787. https://doi.org/10.1016/j.conbuildmat.2019.116787.
Dong, C.Q., Zhang, R.J., Zheng, J.J. and Jiang, W.H. (2020), "Strength behavior of dredged mud slurry treated jointly by cement, metakaolin and flocculant", *Appl. Clay Sci.*, **193**, 105676. https://doi.org/10.1016/j.clay.2020.105676.
Fox, P.J. and Baxter, C.D. (1997), "Consolidation properties of soil slurries from hydraulic consolidation test", *J. Geotech. Geoenviron. Eng.*, **123**(8), 770-776. https://doi.org/10.1061/(ASCE)1090-0241(1997)123:8(770).
Gao, Y.F., Zhang, Y., Zhou, Y. and Li, D.Y. (2016), "Effects of column diameter on setting behavior of dredged slurry in sedimentation experiments", *Mar. Georesour. Geotechnol.*, **34**(5), 431-439. https://doi.org/10.1080/1064119X.2015.1020975.
Hong, Z.S., Yin, J. and Cui, Y.J. (2010), "Compression behaviour of reconstituted soils at high initial water contents", *Geotechnique*, **60**(9), 691-700. https://doi.org/10.1680/geot.09.P.059.
Hong, Z.S., Zeng, L.L., Cui, Y.J., Cai, Y.Q. and Lin, C. (2012), "Compression behaviour of natural and reconstituted clays", *Geotechnique*, **62**(4), 291-301. https://doi.org/10.1680/geot.10.P.046.
Hossain, M. and Chai, J. (2014), "Estimating coefficient of consolidation and hydraulic conductivity from piezocone test results-Case studies", *Geomech. Eng.*, **6**(6), 577-592. https://doi.org/10.12989/gae.2014.6.6.577.
Imai, G. (1979), "Development of a new consolidation test procedure using seepage force", *Soils Found.*, **19**(3), 45-60. https://doi.org/10.3208/sandf1972.19.3_45.
Imai, G. (1981), "Experimental studies on sedimentation mechanism and sediment formation of clay materials", *Soils Found.*, **21** (1), 7-20. https://doi.org/10.3208/sandf1972.21.7.
Jun, S.H., Lee, J.H., Park, B.S. and Kwon, H.J. (2021), "Design charts for consolidation settlement of marine clays using finite strain consolidation theory", *Geomech. Eng.*, **24**(3), 295-305. https://doi.org/10.12989/gae.2021.24.3.295.
Karadoğan, Ü., Korkut, S., Çevikbilen, G., Teymur, B. and Koyuncu, İ. (2021), "Evaluation of beneficial of polyacrylamide use dewatering of dredged sludge obtained from golden horn", *Mar. Georesour. Geotechnol.*, **39**(8), 919-928. https://doi.org/10.1080/1064119X.2020.1780526.
Kim, H.J., Won, M.S., Lee, J.B., Joo, J.H. and Jamin, J.C. (2015), "Comparative study on the behavior of soil fills on rigid acrylic and flexible geotextile containers", *Geomech. Eng.*, **9**(2), 243-259. https://doi.org/10.12989/gae.2015.9.2.243.
Lei, H., Feng, S. and Jiang, Y. (2018), "Geotechnical characteristics and consolidation properties of Tianjin marine clay", *Geomech. Eng.*, **16**(2), 125-140. https://doi.org/10.12989/gae.2018.16.2.125.
Pane, V. and Schiffman, R.L. (1997), "The permeability of clay suspensions", *Geotechnique*, **47**(2), 273-288. https://doi.org/10.1680/geot.1997.47.2.273.
Wu, Y., Kong, G., Lu, Y. and Sun, D.A. (2017), "Experimental study on vacuum preloading with flocculation for solid-liquid separation in waste slurry", *Geomech. Eng.*, **13**(2), 319-331. https://doi.org/10.12989/gae.2017.13.2.319.
Wu, Y., Jiang, H., Lu, Y. and Sun, D. (2019), "Experimental study on treatment of waste slurry by vacuum preloading with different conditioning agents", *Geomech. Eng.*, **17**(6), 543-551. https://doi.org/10.12989/gae.2019.17.6.543.
Xu, G.Z., Gao, Y.F., Hong, Z.S. and Ding, J.W. (2012), "Sedimentation behavior of four dredged slurries in China", *Mar. Georesour. Geotechnol.*, **30**(2), 143-156. https://doi.org/10.1080/1064119X.2011.602382.
Yoobanpot, N., Jamsawang, P., Krairan, K., Jongpradist, P. and Horpibulsuk, S. (2018), "Reuse of dredged sediments as pavement materials by cement kiln dust and lime treatment", *Geomech. Eng.*, **15**(4), 1005-1016. https://doi.org/10.12989/gae.2018.15.4.1005.
Zeng, L.L., Hong Z.S. and Cui, Y.J. (2015), "On the volumetric strain-time curve pattern of dredged clays during primary consolidation", *Geotechnique*, **65**(12), 1023-1028. https://doi.org/10.1680/jgeot.15.T.003.
Zeng, L.L., Hong, Z.S., Tian, W.B. and Shi, J.W. (2018), "Settling behavior of clay suspensions produced by dredging activities in China", *Mar. Georesour. Geotechnol.*, **36**(1), 30-37. https://doi.org/10.1080/1064119X.2016.1274808.
Zeng, L.L., Cai, Y.Q., Cui, Y.J. and Hong, Z.S. (2020a), "Hydraulic conductivity of reconstituted clays based on intrinsic compression", *Geotechnique*, **70**(3), 268-275. https://doi.org/10.1680/jgeot.18.P.096.
Zeng, L.L., Hong, Z.S. and Cui, Y.J. (2020b), "United void index for normalizing virgin compression of reconstituted clays", *Can. Geotech. J.*, **57**(10), 1497-1507. https://doi.org/10.1139/cgj-2019-0507.
Zhang, N., Zhu, W., He, H. and Lv, Y. (2017), "Experimental study on sedimentation and consolidation of soil particles in dredged slurry", *KSCE J. Civ. Eng.*, **21**(7), 2596-2606. https://doi.org/10.1007/s12205-017-0068-1.

GC